Cdc42 induces filopodia by promoting the formation of an IRSp53:Mena complex

Sonja Krugmann*, Ingrid Jordens*, Kris Gevaert‡, Mariëtte Driessens*, Joel Vandekerckhove‡ and Alan Hall*†

Background: The Rho GTPases Rho, Rac, and Cdc42 regulate the organization of the actin cytoskeleton by interacting with multiple, distinct downstream effector proteins. Cdc42 controls the formation of actin bundle-containing filopodia at the cellular periphery. The molecular mechanism for this remains as yet unclear.

Results: We report here that Cdc42 interacts with IRSp53/BAP2α, an SH3 domain-containing scaffold protein, at a partial CRIB motif and that an N-terminal fragment of IRSp53 binds, via an intramolecular interaction, to the CRIB motif-containing central region. Overexpression of IRSp53 in fibroblasts leads to the formation of filopodia, and both this and Cdc42-induced filopodia are inhibited by expression of the N-terminal IRSp53 fragment. Using affinity chromatography, we have identified Mena, an Ena/VASP family member, as interacting with the SH3 domain of IRSp53. Mena and IRSp53 act synergistically to promote filopodia formation.

Conclusion: We conclude that the interaction of Cdc42 with the partial CRIB motif of IRSp53 relieves an intramolecular, autoinhibitory interaction with the N terminus, allowing the recruitment of Mena to the IRSp53 SH3 domain. This IRSp53:Mena complex initiates actin filament assembly into filopodia.

Addresses: *MRC Laboratory for Molecular Cell Biology and Cell Biology Unit, CRC Oncogene and Signal Transduction Group and †Department of Biochemistry and Molecular Biology, University College London, Gower Street, London WC1E 6BT, United Kingdom. ‡Department of Medical Protein Research, Flanders Interuniversity Institute for Biotechnology, Ghent University, K.L. Ledeganckstraat 35, 9000 Ghent, Belgium.

Correspondence: Alan Hall
E-mail: alan.hall@ucl.ac.uk

Background

Small GTPases cycle between an active, GTP-bound and an inactive, GDP-bound state and act as molecular switches to control intracellular signal transduction pathways. Rho, Rac, and Cdc42, three members of the Rho family of small GTPases, regulate a host of cellular responses (reviewed in [1]), the best understood of which are dynamic actin rearrangements. Reorganization of the actin cytoskeleton is crucial for many cellular responses such as phagocytosis, cell movement, and changes in morphology. Rho controls the formation of contractile actin:myosin filaments [2], Rac regulates the formation of lamellipodial protrusions (and membrane ruffles) at the cell periphery [3], while Cdc42 regulates filopodia (microspike) formation also at the cell periphery [4, 5].

Over 30 target proteins have been identified that interact with either Cdc42 or Rac, or both, specifically in their GTP-bound forms (reviewed in [6]). Many, though not all, of these contain a recognizable motif, the Cdc42 and Rac interactive binding or CRIB motif, as part of their Rac/Cdc42 binding domain (RBD) [7, 8]. For two of these targets, Pak and WASP, structural analysis reveals that their interaction with an activated GTPase induces a conformational change, which allows the target protein to participate in additional protein:protein interactions [9–11].

The mechanism by which Cdc42 specifically promotes filopodia formation is still not clear. In vitro, Cdc42 activates an Arp2/3 actin nucleation complex, via an interaction with WASp, to promote actin polymerization [12, 13]. In vivo experiments also point to a central role for WASp in Cdc42-induced filopodia formation [14, 15]. However, the Arp2/3 complex is thought to interact with the sides of preexisting actin filaments and initiate de novo actin nucleation to form branched filament networks, structures that are associated with lamellipodia, but not filopodia [16, 17]. It is likely, therefore, that a variety of other molecules are required to specify the Rac-dependent and the Cdc42-dependent organization and assembly of actin filaments [18].

The SH3 domain-containing adaptor protein IRSp53 was originally identified as a substrate of the insulin receptor kinase in CHO cells [19], and three human splice variants (BAI1AP2, BAP2α, and BAP2) differing in their C termini have been identified. It has been reported by one group that IRSp53 is a Rac target involved in lamellipodia formation [20], while another group suggests that it is a Cdc42 target involved in filopodia formation [21]. The reasons for this discrepancy are not clear.

We report here that, in vivo, IRSp53/BAP2α is a Cdc42 target, and it participates in filopodia formation. We have also identified Mena, an Ena/VASP family protein, as an

Figure 1

IRSp53 interacts with Cdc42 through a partial CRIB motif. **(a)** Flag-tagged, constitutively active Rac or Cdc42 alone or together with Myc-tagged IRSp53 were transiently expressed in COS-7 cells. Lysates were subjected to immunoprecipitations using an antibody against the Flag epitope. GTPases and IRSp53 were detected by immunoblot using anti-Flag antibodies and an antiserum raised against IRSp53. **(b)** Top, a schematic diagram of the IRSp53 domain structure is shown. Below, a panel of IRSp53 truncations, deletions, and point mutations in the partial CRIB motif and SH3 domain are shown. These were designed for expression as GST fusion proteins in *E. coli* or with an N-terminal Myc or Flag epitope tag in mammalian cells. Tags are indicated by ovals. **(c,e)** GST fusion proteins, as indicated on the right-hand side, were applied to a nitrocellulose membrane and overlaid with [^{32}P]GTP-loaded L61Rac or L61Cdc42 as indicated above. After extensive washing, associated GTPases were visualized by autoradiography. **(d)** IRSp53 contains a partial CRIB motif, as shown in this alignment of the IRSp53 amino acid residues 268–280 with other Rac and Cdc42 effectors. Conserved residues are boxed.
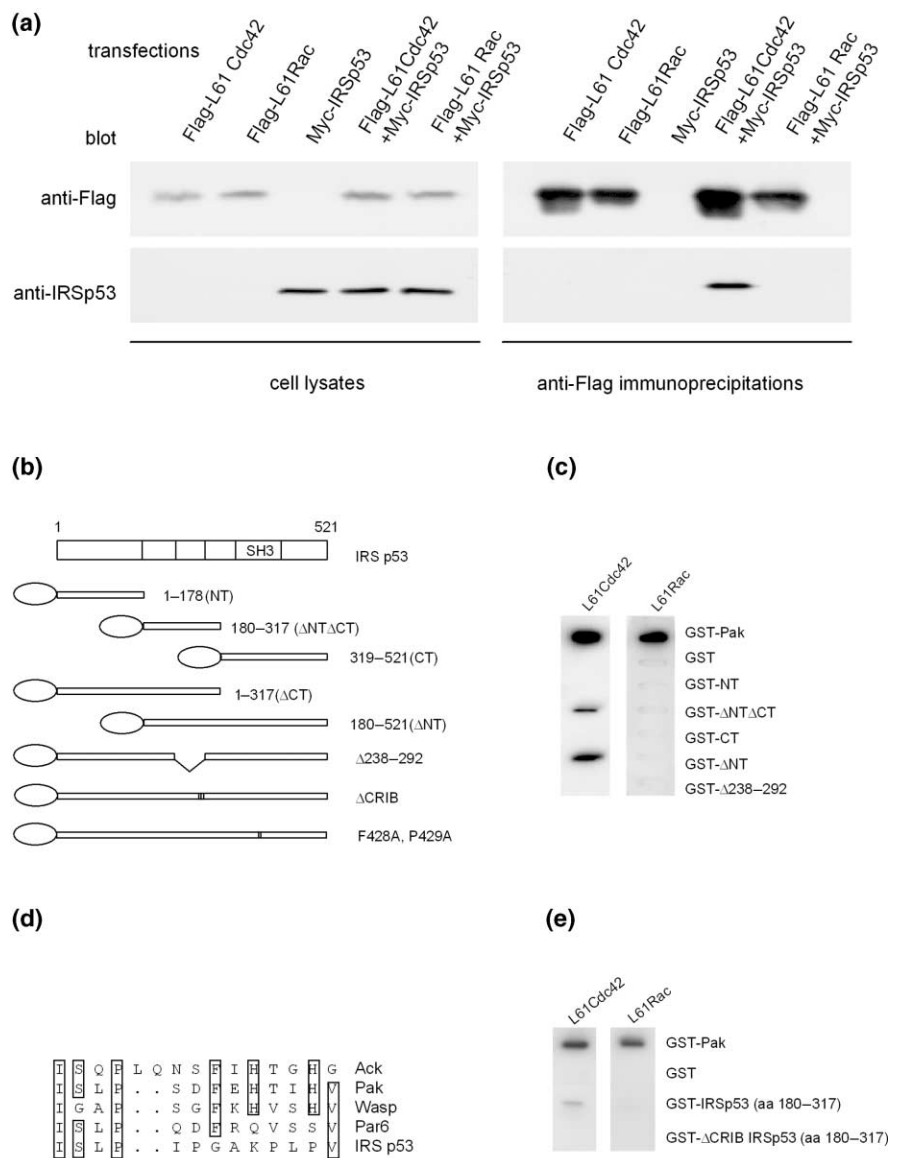
IRSp53 binding protein and find that Mena and IRSp53 act synergistically to promote filopodia formation.

Results

Identification of IRSp53 as a Rho GTPase target

To isolate GTPase targets, a yeast two-hybrid screen with a human cDNA library was performed using activated Rac as bait. One of the Rac-interacting proteins identified was the SH3 domain-containing adaptor protein BAP2α [22], a human ortholog of the previously identified hamster insulin receptor protein kinase substrate IRSp53 [19]. Since some Rac targets are known to interact with other Rho GTPases, Cdc42 and Rho constructs were used as baits in yeast interaction assays. IRSp53 did not interact with Rho, but it interacted with Cdc42 more strongly than with Rac (data not shown).

IRSp53 specifically binds Cdc42 in mammalian cells

To determine the in vivo GTPase binding specificity, COS-7 cells were transfected with IRSp53 along with either constitutively activated Cdc42 (L61Cdc42) or constitutively activated Rac (L61Rac). As shown in Figure 1a, IRSp53 could be coprecipitated from cells with Cdc42, but not with Rac.

The Cdc42 binding site in IRSp53 was mapped using in vitro filter binding assays. Binding of [^{32}P]GTP-loaded Rac and Cdc42 to bacterially expressed IRSp53 fusion

proteins (Figure 1b) was analyzed in an overlay blot assay (Figure 1c). No significant binding of Rac to IRSp53 could be observed using this assay, while L61Cdc42 did interact with IRSp53, albeit significantly weaker than it did with a fragment of p65Pak. A small region of IRSp53 necessary for interaction with Cdc42 was mapped to residues 238–292, and this was found to contain a partial CRIB motif, ISLP(X)$_8$V (amino acids 268–280; Figure 1d). The importance of these residues was confirmed using the triple point mutant I268A, S269A, P271A (ΔCRIB), which abrogated binding of IRSp53 to Cdc42 in the slot blot assay (Figure 1e). We conclude that IRSp53 interacts with Cdc42 through a region containing a partial CRIB motif.

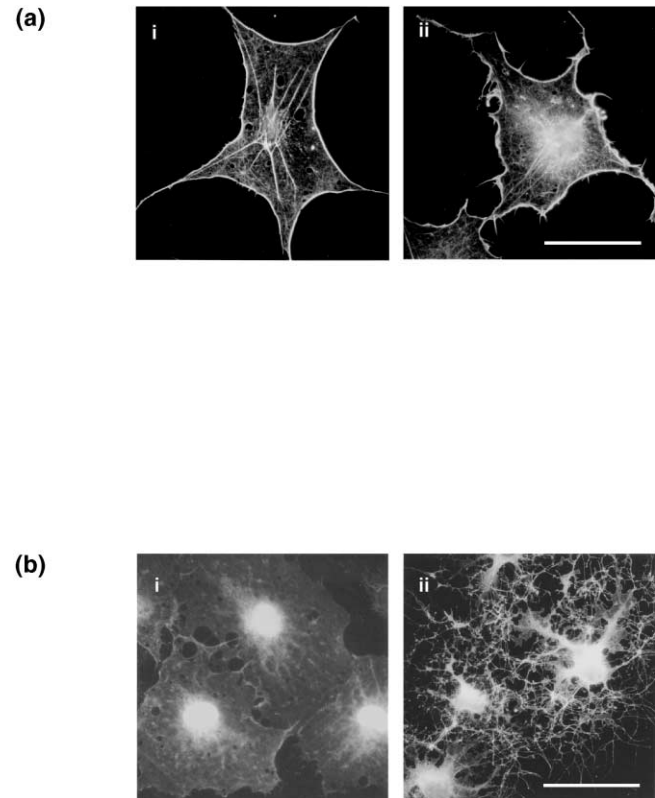## Overexpression of IRSp53 induces filopodia
To determine whether IRSp53 might participate in the regulation of the actin cytoskeleton, subconfluent, quiescent Swiss cells were microinjected with an IRSp53 expression construct. At short expression times (60–100 min), filopodia were clearly induced in 55% of the injected cells, as compared to 3% of the dextran control-injected cells (Figures 2a, panel ii, and 3b, panels i and ii). After longer times (>4.5 hr), expression levels of IRSp53 were higher, and this resulted in severe cell retractions in 90% of the IRSp53-expressing cells (Figures 2b, panel ii, and 3c, panels i and ii). This was confirmed by time-lapse video imaging (data not shown).

Regulation of IRSp53 by Cdc42 and its N terminus
Several Rho GTPase targets have been shown to contain an autoinhibitory region that, through inter- or intramolecular interactions, can prevent additional protein:protein interactions. To test whether IRSp53 contains an autoinhibitory region, we coexpressed combinations of two differently tagged IRSp53 constructs in COS-7 cells and looked for an interaction by coprecipitation. Using this approach, we found that a 178 amino acid fragment derived from the N terminus of IRSp53 (NT IRSp53) was capable of binding to full-length IRSp53 (data not shown). Further analysis, shown in Figure 3a, revealed that this N-terminal fragment interacts with the central region of IRSp53 (ΔNTΔCT IRSp53), encompassing residues 180–317, but not with a C-terminal fragment (CT IRSp53, aa 319–521). This central region contains a relatively proline-rich sequence, the partial CRIB motif, and the Cdc42 binding domain. Full-length IRSp53, in which the CRIB motif is mutated (ΔCRIB IRSp53) and which no longer interacts with Cdc42, still interacts with the N-terminal fragment (data not shown).

To assess whether the N-terminal fragment can inhibit IRSp53 function, it was coexpressed with full-length IRSp53 in quiescent Swiss cells. Expression of full-length IRSp53 alone for 1 hr (Figure 3b, panels i and ii) leads to the formation of filopodia as described above, but this activity was blocked when coexpressed with the N-terminal frag-

(a)

(b)

IRSp53 induces filopodia and cell retraction. **(a)** Quiescent, subconfluent Swiss 3T3 cells were microinjected with (i) biotin dextran as control or with (ii) an expression vector encoding Myc-tagged full-length IRSp53. Cells were fixed 90 min after microinjection and stained for injection markers (data not shown), protein expression (data not shown), and filamentous actin (shown). **(b)** Quiescent, confluent Swiss 3T3 cells were injected as in (a), fixed 4.5 hr after injections, and stained with injection markers (data not shown) and for protein expression (shown). The scale bar represents 20 μm.

ment when only 3% of the injected cells displayed filopodia (Figure 3b, panels iii and iv). Expression of full-length IRSp53 for 4 hr induced severe cell retraction, as already described (Figure 3c, panels i and ii), but, again, this was prevented by coexpression of the N-terminal fragment (Figure 3c, panels iii and iv).

IRSp53 functions downstream of Cdc42 in dynamic actin rearrangements
To investigate whether IRSp53 is required for Cdc42-induced filopodia formation, we made use of the N-terminal autoinhibitory fragment. Quiescent, subconfluent Swiss 3T3 cells were microinjected with an expression vector containing the DH/PH domain of FGD1, a Cdc42-specific guanine nucleotide exchange factor (GEF) [23]. This resulted in the activation of Cdc42 and the formation of filopodia clearly visible in 46% of the FGD1-injected cells (Figure 4a,b) and membrane ruffles and stress fibers

Figure 3

IRSp53 is regulated by an autoinhibitory N terminus. **(a)** Myc-tagged IRSp53 fragments (ΔNTΔCT or CT IRSp53) together with an empty vector or with Flag-tagged NT IRSp53 were transiently expressed in COS-7 cells. Lysates were subjected to immunoprecipitations using an antibody against the Myc epitope. Immunoprecipitated IRSp53 fragments were detected simultaneously by immunoblotting, using antibodies against both the Flag and the Myc epitope tags. Immunoprecipitations were from cells transfected as follows. Lane 1: Flag-NT IRSp53; lane 2: Myc-ΔNTΔCT IRSp53; lane 3: Myc-CT IRSp53; lane 4: Flag-NT IRSp53 and Myc-ΔNTΔCT; lane 5: Flag-NT IRSp53 and Myc-CT IRSp53. **(b)** Quiescent, subconfluent Swiss 3T3 cells were microinjected with an expression vector encoding (i and ii) Myc-tagged full-length IRSp53 or (iii and iv) full-length IRSp53 together with NT IRSp53. Cells were fixed 90 min after injection and stained to visualize epitope tags (data not shown) and filamentous actin (shown). Panels ii and iv represent 5-fold enlargements of i and iii, respectively. **(c)** Quiescent, confluent Swiss 3T3 cells were microinjected with an expression vector encoding (i and ii) Myc-tagged full-length IRSp53 or (iii and iv) full-length IRSp53 together with NT IRSp53. Cells were fixed 4.5 hr after injections and stained to visualize (i and iii) epitope tags and (ii and iv) filamentous actin. The scale bar represents 20 μm.

anti-Myc immunoprecipitations
Western blot: Flag and Myc antibodies

---
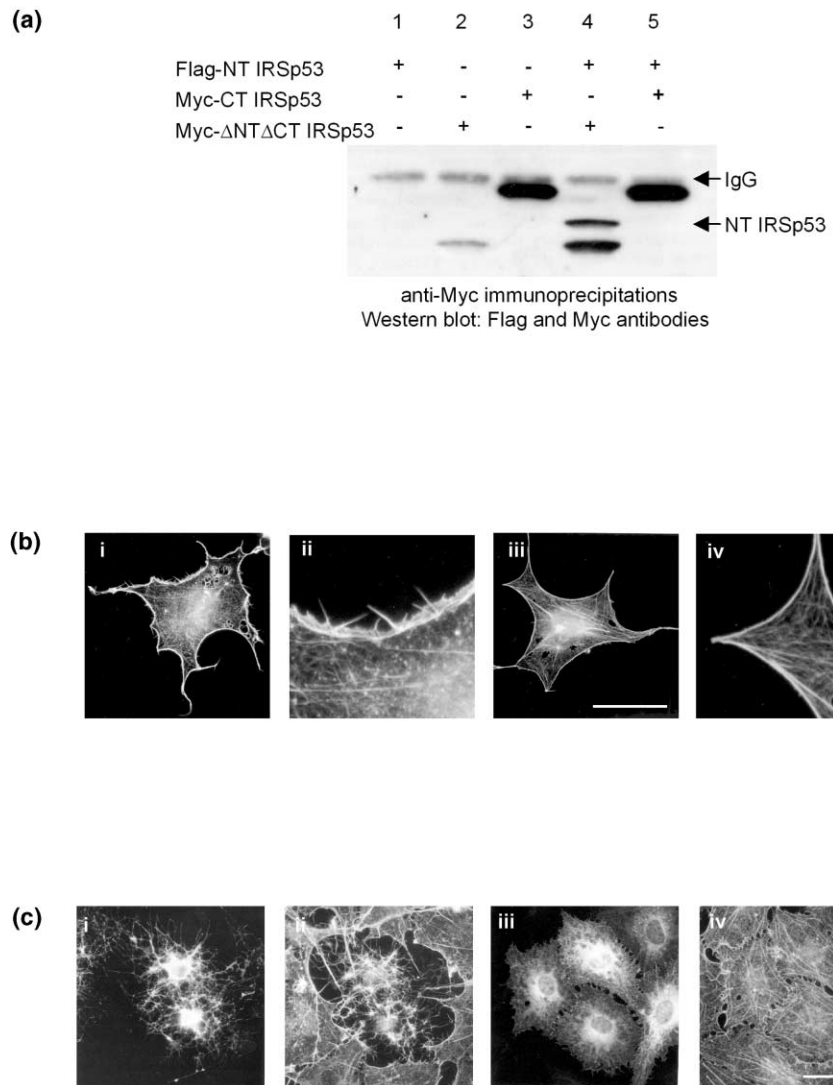
visible in 92% of the FGD1-injected cells (a consequence of subsequent Rac and Rho activation [4]). However, when FGD1 was coexpressed with an N-terminal fragment of IRSp53, filopodia were observed in only 8% of the injected cells (Figure 4c,d), though stress fibers and ruffles were still visible in around 87% of the cells. Expression of the DH/PH domains of Tiam1 (a Rac-specific GEF) led to the formation of membrane ruffles in 85% of the injected cells (Figure 4e), but these were unaffected by coexpression of the N-terminal fragment of IRSp53 (Figure 4f). We conclude that IRSp53 lies downstream of Cdc42 in the pathway leading to filopodia formation but that it is not required for Rac-dependent lamellipodia.

IRSp53 interacts with Mena

To identify cellular components that interact with IRSp53 and might also be involved in the formation of filopodia,

a GST fusion protein of IRSp53 lacking the N-terminal autoinhibitory region (GST-ΔNT IRSp53) was immobilized and used as an affinity matrix. [^{35}S]HeLa cell lysates were incubated with the beads, and eight proteins appeared to interact with GST-ΔNT IRSp53, but not with GST alone (data not shown). This procedure was then scaled up using cell lysates prepared from 4×10^7 HeLa cells and 2.5 μg immobilized GST-IRSp53 fusion protein. After washing, proteins were eluted from the beads in two-dimensional gel electrophoresis sample buffer and separated by two-dimensional gel electrophoresis. Proteins of interest were in gel digested using trypsin, and since MALDI-MS peptide mass fingerprint analysis did not lead to any positive protein identification, the peptide mixture was separated by RP-HPLC, and distinct peptide fractions were analyzed by MALDI-MS. As can be seen in Table 1, one of the proteins was unambiguously identi-

Figure 4

IRSp53 mediates Cdc42-induced formation of filopodia. Quiescent, subconfluent Swiss 3T3 cells were microinjected with an expression vector encoding **(a,b)** epitope-tagged FGD1 DH/PH, **(c,d)** FGD1 DH/PH and NT IRSp53, **(e)** Tiam1 DH/PH, or **(f)** Tiam1 DH/PH and NT IRSp53. Cells were fixed 90 min after injections and stained to visualize epitope tags (data not shown) and filamentous actin (shown). The scale bar represents 20 μm. The images in (b) and (d) are 7.5-fold enlargements of the images in (a) and (c), respectively.
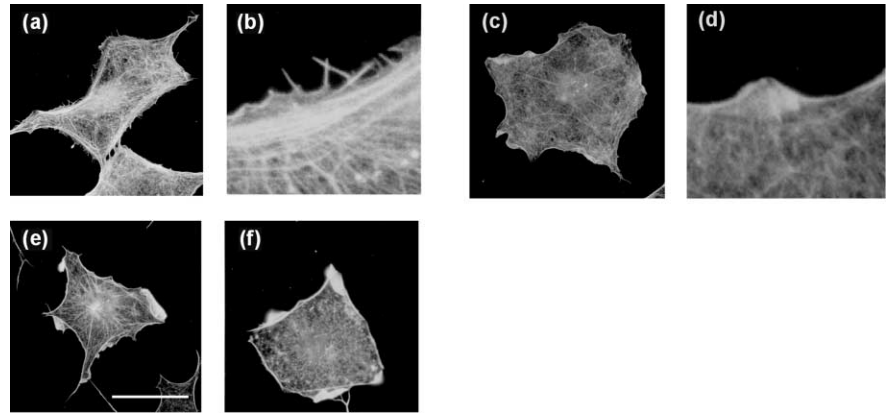
fied as Mena, a member of the Ena/VASP family. Since the complete sequence of human Mena was not available in the public databases at the time of investigation, the obtained peptide mass pattern matched to a human hypothetical protein (database accession number GI:6453482) of only 178 amino acids, which showed very strong similarity to the C-terminal part (amino acids 364–541) of the mouse Mena protein (database accession number GI:1644455). This initial identification was further supported by the matching of other peptide masses to the N-terminal part of the mouse Mena protein (see Table 1a). In total, over 27% of the mouse Mena protein was covered using the obtained peptide masses, thereby univocally identifying this protein.

To confirm this interaction, recombinant GST-ΔNT IRSp53 was immobilized on agarose beads and incubated with in vitro-translated [35S]Mena. After extensive washing, bound proteins were resolved by SDS-PAGE and visual-

ized by autoradiography. Figure 5a, lane 4 shows that Mena interacts directly with GST-ΔNT IRSp53, as does Scar2 (lane 6), as previously reported [20]. Using a slot blot overlay assay (Figure 5b), the interaction of Mena with IRSp53 appeared to be complex; it interacted strongly with the SH3 domain-containing C-terminal part of IRSp53 (aa 319–521; Figure 5b, GST-CT) and weakly to sequences between 180 and 319 (Figure 5b, GST-ΔCT).

The autoinhibitory fragment of IRSp53 and Cdc42 binding regulate the interaction of IRSp53 with Mena

To address whether the autoinhibitory N-terminal fragment of IRSp53 interferes with Mena binding, Myc-tagged ΔNT IRSp53 was first transfected into COS-7 cells with or without a Flag-tagged, N-terminal fragment of IRSp53 (NT IRSp53). Myc-tagged ΔNT IRSp53 was immunoprecipitated with anti-*myc* antibody, the precipitates were incubated with in vitro-translated [35S]Mena, and

Table 1

Mena tryptic peptide masses and sequences.

	$(M + H)^+_{obs}$	Position	Amino acid sequence
(a)			
	1221.52	23–34	WVPAGGSTGFSR
	1579.63	70–81	YNQATQTFHQWR
	1595.66	35–47	VHIYHHTGNNTFR
	1785.21	523–537	LKEELIDAIRQELSK
	2493.24	123–144	QNSQLPAQVQNGPSQEELEIQR
	2649.32	123–145	QNSQLPAQVQNGPSQEELEIQRR
(b)			
	1133.59	455–465	A**S**STSTPEPTR
	1829.88	455–470	A**S**STSTPEPTRKPWER
	2055.94	378–398	**M**ED**T**SFP**S**GGN**AIGV N**SASSK
	2071.91	378–398	**M***ED**T**SFP**S**GGN**AIGV N**SASSK
	2414.18	375–398	VSR**M***ED**T**SFP**S**GGN**AIGV N**SASSK
	2542.08	374–398	KVSR**M***ED**T**SFP**S**GGN**AIGV N**SASSK

Observed peptide masses and their corresponding peptide sequences that match to (a) tryptic peptides present in the mouse Mena protein and to (b) tryptic peptides present in a human hypothetical protein that shows high similarity to the C-terminal part of the mouse Mena protein. Amino acids that differ between the two proteins are shown in bold for the peptides present in the human protein.

Figure 5

(a)

(b)
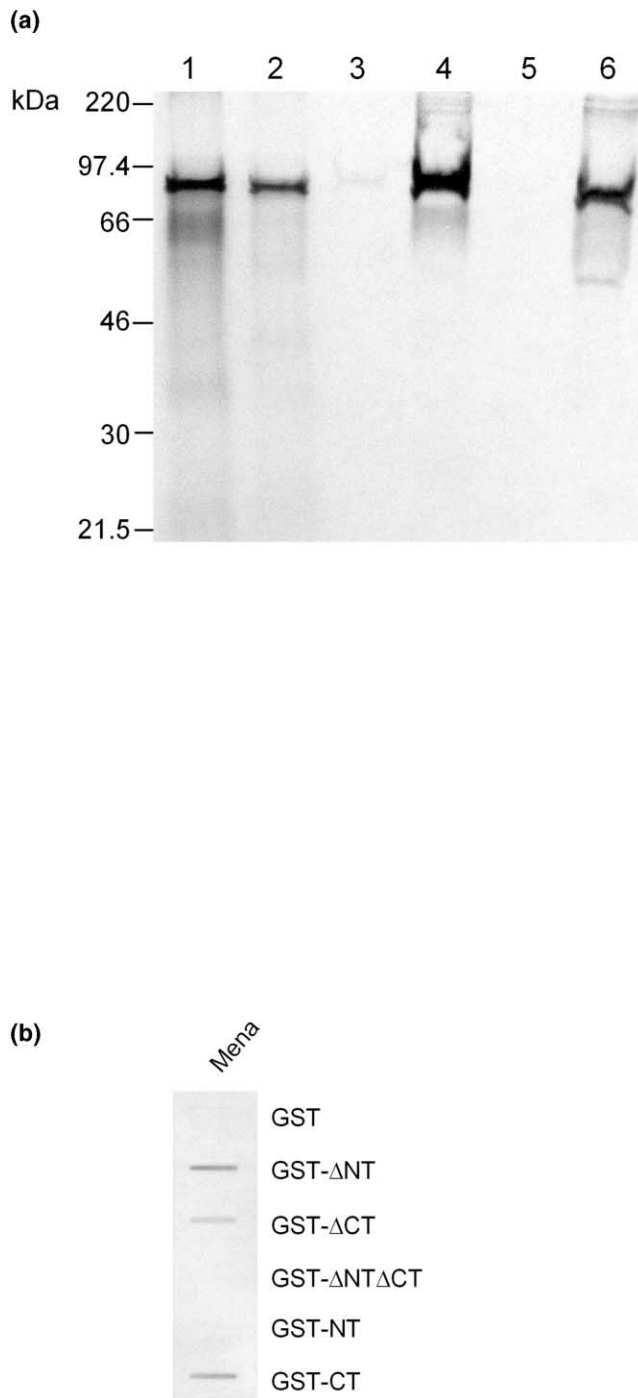
IRSp53 interacts directly with Mena and Scar2. **(a)** In vitro-translated, [^{35}S]Met Mena and Scar2 proteins (lanes 1 and 2) were allowed to interact with (lanes 3 and 5) recombinant GST or (lanes 4 and 6) GST-ΔNT IRSp53 fusion proteins immobilized on glutathione agarose. After extensive washing, proteins were resolved by SDS-PAGE; bound Mena and Scar2 proteins were visualized by autoradiography (lanes 3–6). **(b)** GST fusions of IRSp53 constructs were immobilized on nitrocellulose, as indicated on the right-hand side, and the blot was overlaid with in vitro-translated [^{35}S]Met Mena. After washing, Mena that had associated with the IRSp53 truncations was visualized by autoradiography.

protein complexes were resolved by SDS-PAGE. Precipitated ΔNT IRSp53 and NT IRSp53 were visualized with Coomassie blue (Figure 6a, left panel), and any associated Mena was visualized by autoradiography. As can be seen in the right panel of Figure 6a, coexpression of the N-terminal fragment severely inhibits the interaction of Mena with IRSp53.

To determine whether the interaction between IRSp53 and Mena is regulated by Cdc42, we took advantage of the fact that overexpressed Mena has been previously shown to induce and to localize to F-actin-containing puncta [24, 25]. In agreement with our in vitro binding data, IRSp53 showed a striking colocalization with Mena at these puncta (Figure 6b, panels i and ii). However, an IRSp53 construct with mutations in the CRIB motif (IRSp53 I268A, S269A, P271A [ΔCRIB] triple point mutant) did not associate with Mena-induced puncta (Figure 6b, panels iii and iv). This data suggests that the interaction of IRSp53 with Cdc42 (via the CRIB motif) is required to promote the interaction between IRSp53 and Mena.
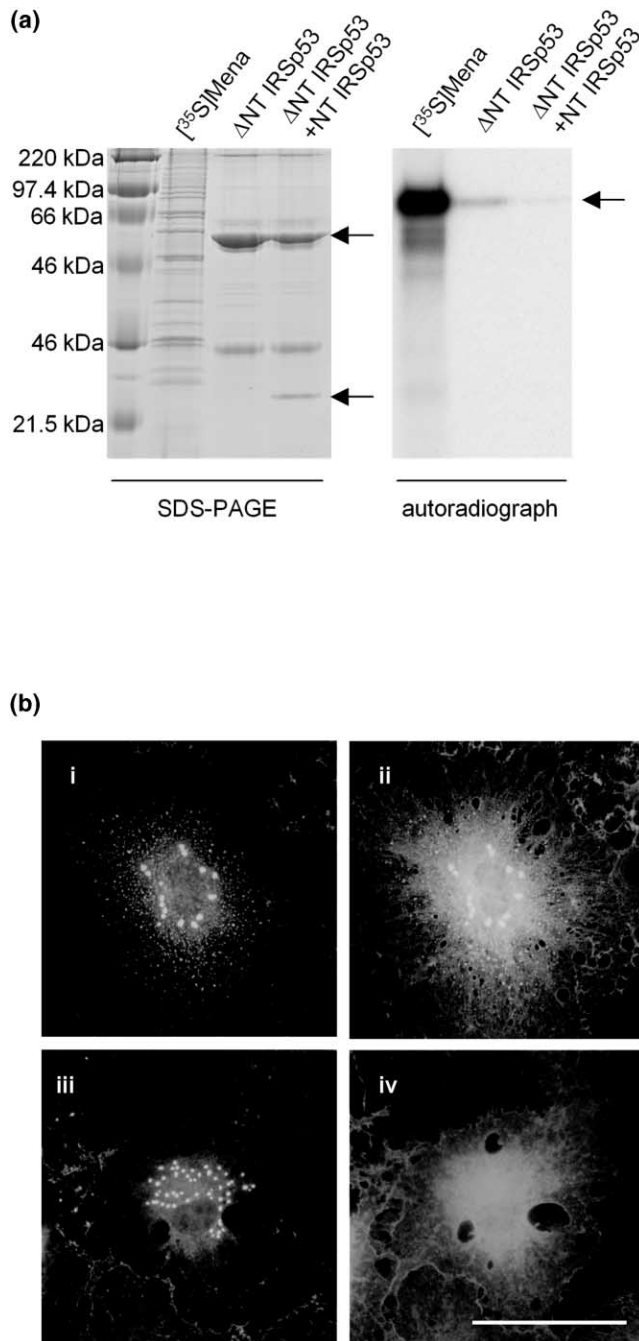
IRSp53 and Mena synergize in vivo to promote filopodia formation

To address the significance of the IRSp53:Mena interaction, Mena was expressed alone or with full-length IRSp53 in quiescent Swiss 3T3 cells. After relatively long expression times (3 hr), 38% of the cells injected with a Mena construct developed some filopodia (Figure 7a), similar to cells expressing IRSp53 alone (Figure 7c). However, coexpression of both Mena and IRSp53 led to a very dramatic phenotype, with 63% of the cells showing dense filopodia structures over the entire cell periphery, even after short expression times (Figure 7b,g shows a Mena- and IRSp53-expressing cell after 90 min).

To confirm that this synergistic effect is dependent on a direct interaction between Mena and IRSp53, Mena was coexpressed with full-length IRSp53 containing two amino acid substitutions (F428A, P429A) in the SH3 domain. This mutant interacts poorly with Mena, and, when expressed alone, it does not induce filopodia. As shown in Figure 7d, the SH3 point mutations abolished the synergistic effects on filopodia formation observed after coexpressing Mena and IRSp53, with 23% of the cells showing a few filopodia.

To determine whether the N-terminal fragment of IRSp53 can interfere with Mena function in vivo, three constructs were coexpressed in Swiss 3T3 cells. As shown in Figure 7e, coexpression of the N-terminal fragment of IRSp53 severely inhibited filopodia formation induced by a combination of Mena and full-length IRSp53.

Finally, to determine whether Cdc42 is required to relieve

Figure 6

(a)

| | [^{35}S]Mena | ΔNT IRSp53 | ΔNT IRSp53 +NT IRSp53 | | [^{35}S]Mena | ΔNT IRSp53 | ΔNT IRSp53 +NT IRSp53 |

220 kDa
97.4 kDa
66 kDa
46 kDa
46 kDa
21.5 kDa

SDS-PAGE   autoradiograph

(b)

i ii iii iv

The N terminus and the CRIB motif of IRSp53 regulate Mena binding to the IRSp53 SH3 domain. **(a)** Myc-tagged ΔNT IRSp53 or Flag-tagged NT IRSp53 and Myc-ΔNT IRSp53 were transiently expressed in COS-7 cells, immunoprecipitated using anti-*myc* antibody-coated sepharose beads, and incubated with in vitro- translated [^{35}S]Met Mena protein. To visualize bait proteins, the gel was stained with Coomassie blue (left panel) prior to exposing for autoradiography to visualize associated Mena (right panel). Molecular weight markers are indicated on the left-hand side. **(b)** Quiescent, confluent Swiss 3T3 cells were microinjected with expression vectors encoding AU-tagged Mena together with (i and ii) full-length, Myc-tagged IRSp53

IRSp53 autoinhibition, a full-length IRSp53 construct containing three amino acid substitutions in the CRIB motif (ΔCRIB IRSp53) was coexpressed with Mena. As seen in Figure 7f, only 12% of the injected cells displayed some filopodia.

Discussion

The data indicate that IRSp53 interacts with Cdc42, but not Rac, in vitro and in vivo in a GTP-dependent manner through a partial CRIB motif. Ectopic expression of IRSp53 caused the formation of filopodia, but not lamellipodia, in Swiss fibroblasts, while IRSp53 harboring a mutated CRIB motif was inactive. This suggests that this protein is a direct Cdc42-regulated target involved in a pathway leading to actin polymerization and filopodia formation. Coexpression of the N-terminal 178 amino acids of IRSp53 inhibited filopodia formation induced by either IRSp53 or Cdc42. We conclude from this that IRSp53, similarly to WASp and p65PAK, two other targets of Cdc42, contains autoinhibitory sequences that interfere with its function. Presumably, there is sufficient GTP-Cdc42 in IRSp53-injected, starved Swiss cells to allow the opening up of some of the IRSp53 and for filopodium formation to occur.

These observations linking IRSp53 to Cdc42 and filopodia are consistent with those published recently by Govind et al. [21], who reported a role for IRS-58, a longer isoform of IRSp53, in neurite outgrowth and filopodia formation in a Cdc42-dependent fashion. However, our findings cannot be easily reconciled with those of Miki et al. [20], who placed IRSp53 downstream of Rac and who argued for a role for IRSp53 in the Rac-dependent formation of lamellipodia in COS-7 cells. Interestingly, Miki and colleagues found that Rac interacted with sequences located in the N-terminal 229 amino acids of IRSp53, not through sequences surrounding the partial CRIB motif. We cannot easily account for these differences, though one possibility is that this group used a different isoform of IRSp53. Apart from IRS-58, three human IRSp53 splice variants differing only in their C termini have so far been reported [22].

To elucidate how IRSp53, upon interaction with Cdc42, leads to filopodia assembly, we have used affinity chromatography techniques coupled to MALDI-MS analysis to look for proteins that interact with the nonautoinhibited form of the protein. Using this approach, we identified an interaction with the Ena/VASP family member Mena. When overexpressed alone, Mena induced some filopodia in Swiss fibroblasts similarly to expression of IRSp53

or (iii and iv) the ΔCRIB IRSp53 point mutant. Cells were fixed 3.5 hr after injections and (i and iii) stained with anti-AU antibody to visualize Mena and with (ii and iv) anti-*myc* antibody to visualize IRSp53. The scale bar represents 20 μm.

Figure 7

Mena and IRSp53 synergize to promote filopodia formation. Quiescent, subconfluent Swiss 3T3 cells were microinjected with an expression vector encoding **(a)** epitope-tagged Mena, **(b,g)** Mena and full-length IRSp53, **(c)** IRSp53, **(d)** Mena and F428A, P429A IRSp53, **(e)** Mena, IRSp53, and NT IRSp53, or **(f)** Mena and ΔCRIB IRSp53. Cells were fixed (b–g) 90 min after injections and (a) 3.5 hr after injection and were stained to visualize epitope tags (data not shown) and filamentous actin (shown). The scale bar represents 20 μm. (g) is a 5-fold enlargement of (b).
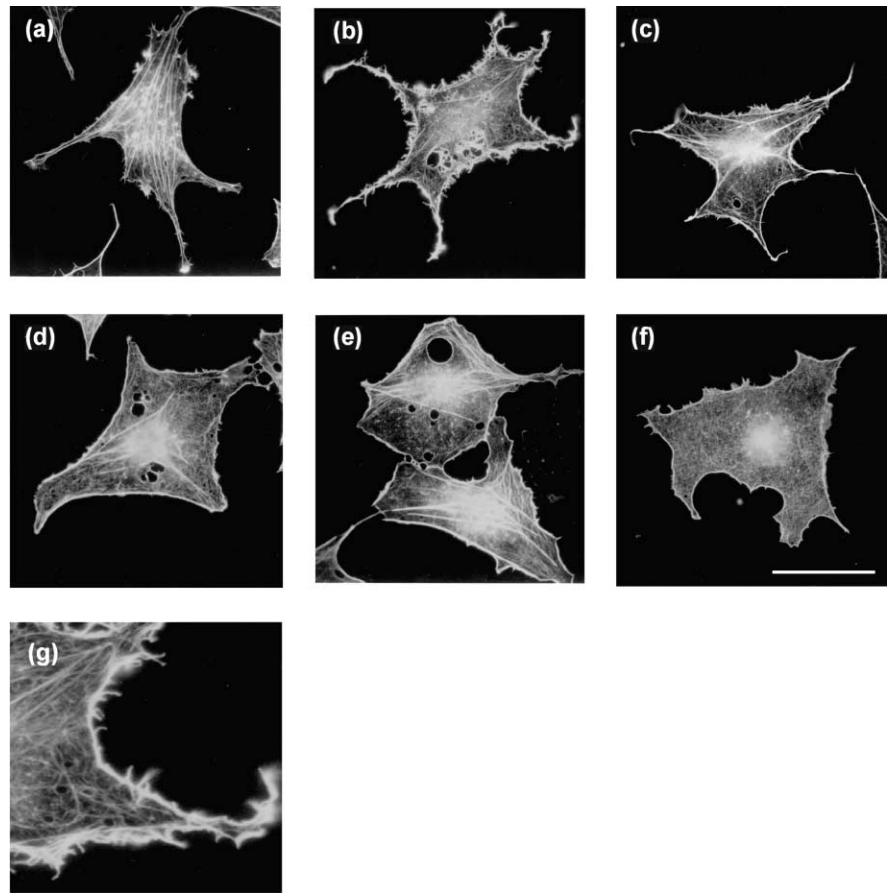

alone. Most strikingly, however, we found that coexpression of Mena and IRSp53 resulted in cells completely covered with actin-rich filopodia. This synergistic activity was abrogated if IRSp53 was unable to interact directly with Mena (through mutation of the SH3 domain in IRSp53) or with Cdc42 (through mutation of the CRIB motif). We conclude that Cdc42-induced filopodia formation is mediated by the assembly of an IRSp53:Mena complex.

The family of Ena/VASP proteins is comprised of Mena, VASP, and Evl in mammalian cells. Mena has been shown to localize to focal adhesion sites through an N-terminal EVH1 (Ena/VASP homology) domain and to the leading edge of lamellipodia and the tips of filopodia [24–27]. In addition, Mena contains proline-rich stretches that interact with profilin and SH3-containing proteins and a C-terminal EVH2 domain that interacts with filamentous actin [24, 25, 28, 29]. Our data suggest that Mena interacts

Figure 8

A schematic model for the regulation of IRSp53 and its interaction with regulation Cdc42 and Mena. In the resting state, the IRSp53 N terminus interacts with the central region of the molecule, and the SH3 domain is masked. In response to an appropriate stimulatory signal, GTP-loaded Cdc42 binds to the CRIB motif. This abrogates the autoinhibitory, intramolecular interaction and allows the SH3 domain to interact with IRSp53 effector proteins such as Mena.
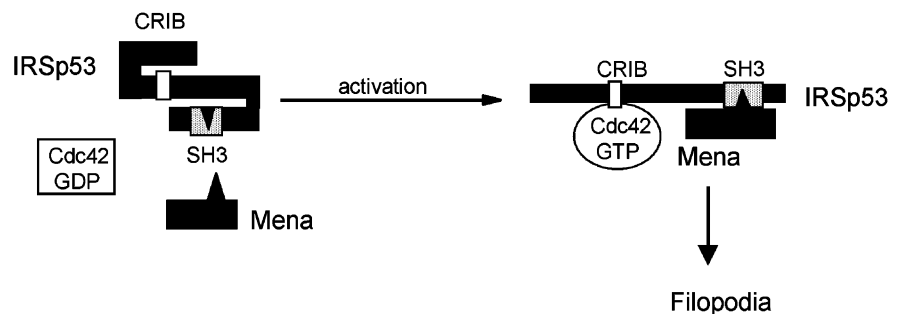
with the SH3 domain of IRSp53, presumably through proline-rich sequences.

The cellular location, along with its involvement in actin-based motility of *Listeria monocytogenes*, strongly suggests that Mena is involved in regulating actin filament dynamics [30, 31]. Its exact role is, however, not clear, and despite playing a positive role in promoting *Listeria* movement, it has been shown to inhibit fibroblast cell motility [32]. Our findings support a key role for a Mena:IRSp53 complex in filopodia formation, and a model for this is shown in Figure 8. These conclusions are in agreement with previous work that has implicated Mena in the formation of adherens junctions in epithelial cells, a process driven by filopodia-mediated cell-cell interactions, and in growth cone guidance, in which filopodia play a central role [33–35]. How the IRSp53:Mena complex promotes actin filament assembly to produce filopodia is not clear, but the localization of Mena to the tips of growing filopodia suggests that, unlike the Arp2/3 complex, it remains associated with the plus ends of growing filaments. Interestingly, IRSp53 is found in abundance at the postsynaptic density (PSD) in neurons in the hippocampus and cerebellum, suggesting that it might play an organizational role in the structure of the PSD, perhaps through its effects on the actin cytoskeleton [36]. Finally, IRSp53 was originally identified as a substrate of the insulin receptor kinase [19], and Ena/VASP proteins are known to be tightly regulated by phosphorylation through cyclic nucleotide-dependent kinases and Abl [37, 38]. It will be interesting to investigate the role of phosphorylation on Cdc42-dependent filopodia formation, and these experiments are currently underway.

Materials and methods

Yeast two-hybrid screen
A human brain cDNA library fused to the GAL4 activation domain in the pACTII vector was screened using human L61Y40CRac1 fused to the GAL4 binding domain in pYTH9 as a bait as previously described [39]. Approximately 5×10^6 colonies were screened on selective medium supplemented with 25 mM 3-aminotriazole. The fastest growing colonies were screened by replating, and, using the LacZ reporter gene assay, their plasmids were isolated and sequenced.

Site-directed mutagenesis
All truncation, deletion, and point mutations in IRSp53 were generated using polymerase chain reaction-based cloning strategies with mutagenic primers and Pfu polymerase (Stratagene). pRK5-AU-Mena was generated by conventional cloning from a retroviral Mena expression construct, which was a kind gift from F. Gertler (Massachusetts Institute of Technology). The pRK5 Scar2 construct was generated from a Scar2 construct, which was kindly provided by Giorgio Scita (European Institute of Oncology).

Cell culture
Swiss 3T3, COS-7, and HeLa cells were grown in Dulbecco's modified Eagle's medium (GIBCO BRL) supplemented with 10% fetal calf serum (Nalgene or Sigma), penicillin, and streptomycin (GIBCO BRL) at 37°C in a humidified atmosphere with 10% CO_2.

Recombinant proteins
All recombinant proteins were expressed as glutathione S-transferase fusions in BL-21 *Escherichia coli* cells and purified on glutathione agarose (Sigma) beads according to standard protocols. GTPases were released from beads by thrombin cleavage; IRSp53 proteins were eluted with 10 mM glutathione (pH 7.5) where applicable. Protein concentrations were determined using a BioRad protein assay kit and purity on SDS-PAGE against BSA as standard; active concentrations of GTPases were determined by filter binding assays as previously described [40].

In vitro translation
Proteins were generated from pRK5 vectors using an in vitro-coupled transcription/translation system (Promega) according to manufacturer's instructions.

Slot blot assays
A total of 10 μg GST-Pak (residues 56–144) and molar equivalent amounts of all other fusion proteins were applied onto nitrocellulose filters using a slot blot apparatus (Hoefer). Filters were probed with 0.5 μg (active concentration) γ-[^{32}P]GTP (NEN)-preloaded GTPases.

Transient transfections of COS-7
Exponentially growing COS-7 cells were transfected using lipofectamine reagent (GIBCO BRL) according to the manufacturer's instructions with a total of 1 μg plasmid DNA (the total amount was made up to 1 μg with empty vector DNA where applicable in control transfections). A total of 30 hr after transfecting, cells were lysed in 1× PBS, 1 mM $MgCl_2$, 1mM EGTA, and 1% Triton X-100. Cytoplasmic fractions were immunoprecipitated with 10 μl packed, covalently coupled anti-*myc* antibody sepharose beads, followed by extensive washes in lysis buffer. For pull-down experiments, lysates were incubated with GST fusion constructs immobilized on GST agarose. After extensive washing, beads were boiled in sample buffer, and proteins were resolved by SDS-PAGE and wet blotted onto polyvinylidene fluoride membranes (Millipore). Proteins were immunoblotted using appropriate antibodies.

Microinjection
For microinjections, Swiss 3T3 cells were seeded at high density (4 × 10^5 cells per 13-mm glass coverslip) into Dulbecco's modified Eagle's medium supplemented with 4% fetal calf serum and left to quiesce for 10 days; quiescent cells were serum starved for 16 hr immediately prior to injections. To prepare subconfluent, quiescent Swiss 3T3 cells, 2 × 10^6 cells were seeded into a 6-cm dish into Dulbecco's modified Eagle's medium supplemented with 4% fetal calf serum and left until quiescent. A total of 20 hr prior to injecting, the cells were trypsinized in 0.5 ml cold trypsin, which was subsequently inhibited using soybean trypsin inhibitor (Sigma). Cells were washed in serum-free medium before being plated onto fibronectin-coated coverslips (at a density of 1.5 × 10^4 cells per coverslip). On each coverslip, 100–150 cell nuclei were microinjected over a period of 15 min in a temperature- and CO_2-controlled chamber. Eukaryotic expression vectors were diluted in PBS (0.1 mg/ml with the exception of IRSp53, which was 0.05 mg/ml; for coinjections, the total DNA concentration was made up to 0.1 mg/ml with empty vector). Control cells were injected with 2 mg/ml biotin dextran. After injections, coverslips were returned to the incubator to allow cells to recover and express proteins.

Antibodies
IRSp53 antisera were raised in rabbits against recombinant, thrombin-cleaved fragments (1–178 and 180–317) of IRSp53 (Cocalico Biologicals). Antibodies used to detect epitope tags were anti-*myc* 9E10 crude hybridoma supernatant or rat JAC6 (a kind gift from R. Marais, Institute of Cancer Research), anti-Flag M2 (Sigma), and anti-AU ascites fluid (BABCO). Secondary, fluoresceine-, rhodamine-, or alexa-coupled antibodies were from Jackson ImmunoResearch Laboratories. Biotin-dextran was detected with fluoresceine-coupled streptavidin (Amersham); filamentous actin was visualized with rhodamine-phalloidin (Molecular Probes). HRP conjugates were from Pierce.

Immunofluorescence staining
Cells were fixed in 4% paraformaldehyde in PBS, permeabilized with 0.2% Triton X-100 in PBS, and blocked in 0.5 mg/ml sodium borohydrate in PBS. For visualization of actin filopodia, cells were fixed in 4% para-formaldehyde and 0.5% glutaraldehyde; in this case, all cells were coinjected with biotin-dextran as an injection marker. After staining with appropriate reagent, coverslips were mounted onto small drops of moviol mountant containing *p*-phenylenediamine as an antifade agent. Cells were examined on a Zeiss axiophot microscope using $40\times$ and $63\times$ 1.4 oil immersion lenses. Fluorescent images were recorded on Kodak T-Max 400ASA film.

Isolation of IRSp53 binding proteins
Following 16 hr of metabolic labeling with 0.5 mCi [^{35}S]Cys, Met-Express (NEN) in cysteine- and methionine- free DMEM (ICN), 1×10^7 HeLa cells were lysed by scraping into 1.5 ml 25 mM HEPES (pH 7.4) (4°C), 1% Triton X-100, 150 mM NaCl, 5 mM EDTA, 0.1 mM EGTA, 1 mM PMSF, and 10 µg/ml each of leupeptin, aprotinin, antipain, and pepstatin A and incubating on ice for 5 min. Insoluble material was pelleted by centrifugation, and the soluble material was incubated with 1 µg GST-ΔNT IRSp53 fusion protein immobilized on 15 µl packed GST agarose beads for 1 hr end-on-end (4°C). After four washes in lysis buffer, beads were boiled in sample buffer, and proteins were resolved by SDS-PAGE. Protein bands were visualized by silver staining and autoradiography. For scale-up preparations, proteins from 4×10^7 cells were resolved on a first dimension 7.5% 16-BAC (benzyldimethyl-*n*-hexadecylammonium chloride)-PAGE gel, essentially as previously described [41]. In brief, gels were poured as described, but the 16-BAC was omitted. Wells were rinsed in running buffer (2.5 mM 16-BAC, 150 mM glycine, 50 mM phosphoric acid), and beads were incubated for 30 min at 37°C in freshly made sample buffer (1.13 g Urea, 0.5% 16-BAC, 300 µl 87% glycerol, 187 µl 1 M DTT per 5 ml) prior to loading the gel; samples were run toward the cathode at 25 mA. Fixing and staining of 16-BAC gels was performed as previously described. Stained gels were equilibrated in 0.1 M Tris-HCl (pH 6.8); protein-containing lanes were excised and inserted onto a second dimension 8% SDS gel with flush top. Gel slices were fixed in place by overlaying with molten 65 mM Tris-HCl (pH 6.8), 30% glycerol, 3% SDS, 0.4% agarose and covered in $1\times$ sample buffer. Gels were stained in brilliant blue G250, and spots of interest were excised for MALDI TOF.

Mass spectrometry
All MALDI-MS measurements were performed on a Bruker Reflex III MALDI mass spectrometer equipped with a delayed ion extraction device (Bruker Daltonics). Proteins of interest were in gel-digested with trypsin using a previously described protocol [42, 43]. A small fraction of each peptide mixture was purified and concentrated on Poros 50 R2 beads and used for peptide mass fingerprint analysis (for technical details, see [42, 43]). Since only minor ion signals were observed in each of the obtained spectra, no unambiguous protein identification could be made. Therefore, the remainder of the peptide mixture was separated by RP-HPLC on a 2.1-mm i.d. $\times$ 50 mm C18-column (Vydac Separations Group) using a steep gradient of acetonitrile. Eluting peptides were automatically collected in a suspension of Poros 50 R2 beads, dried to complete dryness in a centrifugal vacuum concentrator, and used for MALDI-MS analysis [43]. The obtained peptide masses were used to identify the protein using the MASCOT-algorithm available at http://www.matrixscience.com.

References
1. Hall A: **Rho GTPases and the actin cytoskeleton.** *Science* 1998, **279:**509-514.
2. Ridley AJ, Hall A: **The small GTP-binding protein rho regulates the assembly of focal adhesions and actin stress fibers in response to growth factors.** *Cell* 1992, **70:**389-399.
3. Ridley AJ, Paterson HF, Johnston CL, Diekmann D, Hall, A: **The small GTP-binding protein rac regulates growth factor-induced membrane ruffling.** *Cell* 1992, **70:**401-410.
4. Nobes CD, Hall A: **Rho, Rac and Cdc42 GTPases regulate the assembly of multimolecular focal complexes associated with actin stress fibers, lamellipodia, and filopodia.** *Cell* 1995, **81:**53-62.
5. Kozma R, Ahmed S, Best A, Lim L: **The Ras-related protein Cdc42Hs and bradykinin promote formation of peripheral actin microspikes and filopodia in Swiss 3T3 fibroblasts.** *Mol Cell Biol* 1995, **15:**1942-1952.
6. Bishop AL, Hall AL: **Rho GTPases and their effector proteins.** *Biochem J* 2000, **348:**241-255.
7. Burbelo PD, Drechsel D, Hall A: **A conserved binding motif defines numerous candidate target proteins for both Cdc42 and Rac GTPases.** *J Biol Chem* 1995, **270:**29071-29074.
8. Symons M, Derry JMJ, Karlak B, Jiang S, Lemahieu V, McCormick F, *et al.*: **Wiskott-Aldrich syndrome protein, a novel effector for the GTPase CDC42Hs, is implicated in actin polymerization.** *Cell* 1996, **84:**723-734.
9. Kim AS, Kakalis LT, Abdul-Manan N, Liu GA, Rosen MK: **Autoinhibition and activation mechanism of the Wiscott-Aldrich syndrome protein.** *Nature* 2000, **404:**151-158.
10. Lei M, Lu W, Meng W, Parrini MC, Eck M, Mayer BJ, *et al.*: **Structure of Pak1 in an autoinhibited conformation reveals a multistep activation switch.** *Cell* 2000, **102:**387-397.
11. Hoffman GR, Cerione RA: **Flipping the switch: the structural basis for signaling through the CRIB motif.** *Cell* 2000, **102:**403-406.
12. Machesky LM, Insall RH: **Scar1 and the related Wiscott-Aldrich syndrome protein, WASp, regulate the actin cytoskeleton through the Arp2/3 complex.** *Curr Biol* 1998, **8:**1347-1456.
13. Rohatgi R, Ho HY, Kirschner MW: **Mechanism of N-WASP activation by CDC42 and phosphatidylinositol 4,5-bisphosphate.** *J Cell Biol* 2000, **150:**117-120.
14. Miki H, Sasaki T, Takai Y, Takenawa T: **Induction of filopodium formation by a WASP-related actin depolymerizing protein N-WASP.** *Nature* 1998, **391:**93-96.
15. Castellano F, Montcourrier P, Guillemot JC, Gouin E, Machesky L, Cossart P, *et al.*: **Inducible recruitment of Cdc42 or WASp to a cell surface receptor triggers actin polymerization and filopodium formation.** *Curr Biol* 1999, **9:**351-360.
16. Mullins RD, Heuser JA, Pollard TD: **The interaction of Arp2/3 complex with actin: nucleation, high affinity pointed end capping and formation of branched networks of filaments.** *Proc Natl Acad Sci USA* 1998, **6:**6181-6186.
17. Svitkina TM, Borisy GG: **Arp2/3 complex and actin depolymerizing factor/cofilin in dendritic organization and treadmilling of actin filament array in lamellipodia.** *J Cell Biol* 1999, **145:**1009-1026.
18. Martinez-Quiles N, Rohatgi R, Anton IM, Medina M, Saville SP, Miki H, *et al.*: **WIP regulates N-WASP-mediated actin polymerization and filopodium formation.** *Nat Cell Biol* 2001, **3:**484-491.
19. Yeh TC, Ogawa W, Danielsen AG, Roth RA: **Characterization and cloning of a 58/53-kDa substrate of the insulin receptor tyrosine kinase.** *J Biol Chem* 1996, **271:**2921-2928.
20. Miki H, Yamaguchi H, Suetsugu S, Takenawa T: **IRSp53 is an essential intermediate between Rac and WAVE in the regulation of membrane ruffling.** *Nature* 2000, **408:**732-735.
21. Govind S, Kozma R, Monfries C, Lim L, Ahmed S: **Cdc42Hs facilitates cytoskeletal reorganization and neurite outgrowth by localizing the 58-kD insulin receptor substrate to filamentous actin.** *J Cell Biol* 2001, **152:**579-594.
22. Oda K, Shiratsuchi T, Nishimori H, Inazawa J, Yoshikawa H, Taketani Y, *et al.*: **Identification of BAIAP2 (BAI-associated protein2), a novel human homologue of hamster IRSp53, whose SH3 domain interacts with the cytoplasmic domain of BAI1.** *Cytogenet Cell Genet* 1999, **84:**75-82.
23. Nagata K, Driessens M, Lamarche N, Gorski J, Hall A: **Activation of G1 progression, JNK MAP kinase and actin filament**

assembly by the exchange factor FGD1. *J Biol Chem* 1998, **273:**15453-15457.

24. Niebuhr K, Ebel F, Frank R, Reinhard M, Domann E, Carl UD, *et al.*: **A novel proline-rich motif present in ActA of *Listeria monocytogenes* and cytoskeletal proteins is the ligand for the EVH1 domain, a protein module in the Ena/VASP family.** *EMBO J* 1997, **16:**5433-5444.

25. Gertler FB, Niebuhr K, Reinhard M, Wehland J, Soriano P: **Mena, a relative of VASP and *Drosophila* Enabled, is implicated in the control of microfilament dynamics.** *Cell* 1996, **87:**227-239.

26. Lanier LM, Gates MA, Witke W, Menzies AS, Wehmann AM, Macklis JD, *et al.*: **Mena is required for neurolation and commissure formation.** *Neuron* 1999, **22:**313-325.

27. Goldberg DJ, Foley MS, Tang D, Graham PW: **Recruitment of the Arp2/3 complex and Mena for the stimulation of actin polymerization in growth cones by nerve growth factor.** *J Neurosci Res* 2000, **60:**458-467.

28. Bachmann C, Fischer L, Walter U, Reinhard M: **The EVH2 domain of the vasodilator-stimulated phosphoprotein mediates tetramerization, F-actin binding and actin bundle formation.** *J Biol Chem* 1999, **274:**23549-23557.

29. Ermekova KS, Zambrano N, Linn H, Minopoli G, Gertler F, Russo T, *et al.*: **The WW domain of neural protein FE65 interacts with proline-rich motifs in Mena, the mammalian homolog of *Drosophila* Enabled.** *J Biol Chem* 1997, **272:**32869-32877.

30. Chakraborty T, Ebel F, Domann E, Niebuhr K, Gerstel B, Pistor S, *et al.*: **A focal adhesion factor directly linking intracellularly motile *Listeria monocytogenes* and *Listeria ivanovii* to the actin-based cytoskeleton of mammalian cells.** *EMBO J* 1995, **14:**1314-1321.

31. Laurent V, Loisel TP, Harbeck B, Wehman A, Gröbe L, Jockusch BM, *et al.*: **Role of proteins of the Ena/VASP family in actin-based motility of *Listeria monocytogenes*.** *J Cell Biol* 1999, **144:**1245-1258.

32. Bear JE, Loureiro JJ, Libova I, Fässler R, Wehland J, Gertler FB: **Negative regulation of fibroblast motility by Ena/VASP proteins.** *Cell* 2000, **101:**717-728.

33. Vasioukhin V, Bauer C, Yin M, Fuchs E: **Directed actin polymerization is the driving force for epithelial cell-cell adhesion.** *Cell* 2000, **100:**209-219.

34. Gertler FB, Doctor SJ, Hoffmann FM: **Genetic suppression of mutations in the *Drosophila* abl proto-oncogene homolog.** *Science* 1990, **248:**857-860.

35. Jay DG: **The clutch hypothesis revisited: ascribing the roles of actin-associated proteins in filopodial protrusions in the nerve growth cone.** *J Neurobiol* 2000, **44:**114-125.

36. Abbott MA, Wells DG, Fallon JR: **The insulin receptor tyrosine kinase substrate p58/53 and the insulin receptor are components of CNS synapses.** *J Neurosci* 1999, **19:**7300-7308.

37. Lambrechts A, Kwiatkowski A, Lanier LM, Bear JE, Vandekerckhove J, Ampe C, *et al.*: **PKA phosphorylation of EVL, a Mena/VASP relative, regulates its interaction with actin and SH3-domains.** *J Biol Chem* 2000, **275:**36143-36151.

38. Comer AR, Ahern-Djamali SM, Juang JL, Jackson PD, Hoffmann FM: **Phosphorylation of Enabled by the *Drosophila* Abelson tyrosine kinase regulates the in vivo function and protein-protein interactions of Enabled.** *Mol Cell Biol* 1998, **18:**152-160.

39. Aspenström P, Olson MF: **Yeast two hybrid system to detect protein-protein interactions with rho GTPases.** *Methods Enzymol* 1995, **256:**228-241.

40. Self AJ, Hall A: **Measurements of intrinsic nucleotide exchange and GTP hydrolysis rates.** *Methods Enzymol* 1995, **256:**67-76.

41. Hartinger J, Stenius K, Högemann D, Jahn R: **16-BAC/SDS-PAGE: a two-dimensional gel electrophoresis system suitable for the separation of integral membrane proteins.** *Anal Biochem* 1996, **240:**126-133.

42. Gevaert K, Demol H, Puype M, Broekaert D, De Boeck S, Houthaeve T, *et al.*: **Peptides adsorbed on reverse-phase chromatographic beads as targets for femtomole sequencing by post-source decay matrix assisted laser desorption ionization-reflectron time of flight mass spectrometry (MALDI-RETOF-MS).** *Electrophoresis* 1997, **18:**2950-2960.

43. Gevaert K, Demol H, Sklyarova T, Vandekerckhove J, Houthaeve T: **A peptide concentration and purification method for protein characterization in the subpicomole range using matrix assisted laser desorption/ionization-postsource decay (MALDI-PSD) sequencing.** *Electrophoresis* 1998, **19:**909-917.